

Atomic structure and edge magnetism in MoS_{2+x} parallelogram shaped platelets†

Cite this: *Phys. Chem. Chem. Phys.*, 2013, **15**, 13077

J. Karthikeyan,^a Vijay Kumar^{bc} and P. Murugan^{*a}

The structural, electronic, and magnetic properties of MoS_{2+x} parallelogram shaped platelets having m and n Mo atoms on the adjoining edges have been studied using first principles calculations and by varying m and n from 1 to 6. These platelets have 100% S coverage on two adjoining edges while 50% S coverage on the other two edges. The structural stability of the platelets increases with size but the highest occupied molecular orbital–lowest unoccupied molecular orbital (HOMO–LUMO) energy gap in general decreases. There is a triangular metallic corner at the intersection of 100% S covered edges of the platelets when $m = n$. On the other hand magnetism is observed on the 50% S covered edges of the platelets for the sizes greater than that of the (3,4) platelet. The magnetic moments mainly arise from the undercoordinated S(2c) atoms at the 50% S covered edges rather than from Mo atoms. The criteria for the existence of the magnetic moments on S(2c) atoms are suggested and the electronic structure of the platelets on the edges as well as inside is discussed.

Received 9th April 2013,
Accepted 28th May 2013

DOI: 10.1039/c3cp51499d

www.rsc.org/pccp

1 Introduction

The discoveries of carbon nanostructures, such as zero dimensional (0-D) C₆₀ and other fullerenes, 1-D carbon nanotubes (CNTs), and 2-D graphene¹ have accelerated research on nanoscale materials as they exhibit fascinating electronic,² mechanical,³ magnetic,⁴ and optical properties⁵ that are size and shape dependent. For example, CNTs can be metallic or semiconducting. On the other hand graphene has exceptionally high mobility which is very attractive but it lacks a band gap that is required for electronic device applications. Many studies have been performed on graphene nanoribbons that can be semiconducting depending upon the edges, but a controlled treatment of edges is a problem. Metal chalcogenides such as MoS₂ are also layered materials similar to graphite, and their nanostructures are considered as the best alternative to those of carbon because chalcogenides have the advantage of making specific structures and moreover bulk MoS₂ has a band gap of 1.2 eV but it is *indirect*. However very interestingly, one layer of MoS₂ has a wider and *direct* band gap⁶ of 1.8 eV. It makes such layers interesting for photovoltaic and light emitting applications,⁷ apart from applications in catalysis⁸ and

solid state lubrication.⁹ Also, 1-D MoS₂ nanoribbons resembling graphene nanoribbons have been synthesized.¹⁰

Among the 0-D nanostructures of MoS₂, single layer thick MoS_{2+x} platelets with different shapes such as triangle^{11,12} and hexagon^{13,14} have been recently synthesized on different substrates. Triangular platelets with different (50% and 100%) coverages of S on their edges were obtained in experiments performed on a Au(111) substrate.^{11,12} The edges of the triangular platelets have interesting catalytic properties for desulfurization of petroleum products. First principle calculations have been performed on these platelets and it has been shown that the binding energies of large sized triangular platelets with 50% and 100% S covered edges are nearly equal.¹¹ The stability of platelets is highly dependent on the coordination number of Mo atoms on the edges¹⁵ and in both such platelets, the Mo atoms have a six coordination as in the bulk. These platelets are formed in an environment of excess sulfur that leads to higher stoichiometry of S on the edges. By controlling the sulfur content, platelets with different types of edges as well as shapes can be formed.

Among the MoS₂ platelets, triangular platelets have been well studied. On the other hand although parallelogram shaped platelets have also been observed, their structural stability has not been studied so far. Developing an understanding of their structure and properties is important as these platelets can be viewed in two ways: (1) a truncated form of MoS₂ ribbon or sheet, and (2) a combination of two triangular platelets where one side has 50% S coverage on the edges while the other has

^a CSIR Central Electrochemical Research Institute, Karaikudi - 630 006, Tamil Nadu, India. E-mail: murugan@cecri.res.in

^b Dr Vijay Kumar Foundation, 1969 Sector 4, Gurgaon 122 001, Haryana, India

^c Center for Informatics, School of Natural Sciences, Shiv Nadar University, Chithera, Gautam Budh Nagar 203 207, Uttar Pradesh, India

† Electronic supplementary information (ESI) available. See DOI: 10.1039/c3cp51499d

100% S covered edges. The present study is focused on the understanding of the structural, electronic, and (edge) magnetic properties of such parallelogram shaped MoS_{2+x} platelets with different (m,n) values, m and n being the numbers of Mo atoms on the two adjoining sides of a parallelogram platelet. Our calculations reveal the occurrence of magnetism in platelets when the size of the platelet is greater than or equal to that of the (3,5) platelet. Most significantly the magnetic moments are distributed mainly on two coordinated $\text{S}(2c)$ atoms, rather than on Mo atoms. Such S atoms are located on edges covered with 50% S. A similar finding of the magnetic moment on S atoms has been reported^{16,17} recently. The origin of magnetism on $\text{S}(2c)$ atoms is understood and it is shown to mainly arise due to fractional charge transfer from Mo to such $\text{S}(2c)$ atoms. Importantly, S atoms on the edges (below and above the plane of the Mo atoms) have a tendency to dimerize and magnetism depends on the separation between the two $\text{S}(2c)$ atoms in the direction perpendicular to the platelet.

In Section II, we present our method of calculations while the results are discussed in Section III. A summary of results is given in Section IV.

2 Computational method

We studied MoS_{2+x} parallelogram shaped platelets of different sizes by calculating their structural and electronic properties using first principles approach within the framework of density functional theory as implemented in the Vienna *Ab-initio* Simulation Package (VASP).¹⁸ The electron-ion interaction potential is represented by projector augmented wave (PAW) pseudopotentials¹⁹ and the exchange–correlation functional is treated within a generalized gradient approximation.²⁰ The energy has been minimized by carrying out iterative electronic minimization and ionic relaxation until the absolute value of force on each ion becomes less than $0.01 \text{ eV } \text{Å}^{-1}$. Since we are interested in studying the platelets of MoS_2 , we considered our initial atomic arrangements as one of a single layer of MoS_2 . First we performed non-spin-polarized calculations on platelets. Subsequently, spin-polarized solutions were obtained. The platelet was placed in a large unit cell with dimensions sufficient to have negligible interaction between the platelet and its periodic images. The Brillouin zone (BZ) was sampled by only the Γ point. To further understand the origin of magnetism in platelets, $\text{MoS}_{2+x}(m, \infty)$ infinite nanoribbons corresponding to (m,n) platelets have been studied by considering periodicity along the y -axis and its lattice constant has been optimized. In the case of nanoribbons the BZ has been sampled by $1 \times 32 \times 1$ Monkhorst–Pack k -points.

3 Results and discussion

Each layer of MoS_2 bulk consists of three sub-atomic layers such that the Mo atomic layer is sandwiched in between two S atomic layers. These three layers are strongly bonded with each other *via* s–p–d hybridization²¹ while such a comprised layer is connected with neighboring layers through van der Waal's

interaction by keeping the interlayer S–S distance of 3.48 Å . Atomically, each Mo atom is surrounded by six S atoms in a trigonal prismatic environment with acute and obtuse S–Mo–S angles of 82° and 136° , respectively.²¹ Further, in this environment, the Mo 4d energy levels split into three, *viz.* a_1 , e' , and e'' sub-groups. They are composed of d_{z^2} , (d_{xz}, d_{yz}) , and $(d_{xy}, d_{x^2-y^2})$ orbitals, respectively.²² However, this symmetry is broken when the layer is cleaved to form various shaped platelets. As a consequence, different electronic and magnetic properties are obtained in these platelets, in contrast to bulk.²³

We studied parallelogram shaped platelets of different sizes to understand the variation in their physical properties as a function of size. In general, the edges of the platelets can be constructed with different S coverage. Notably, 50% S and 100% S covered edges are obtained by cleaving a MoS_2 layer to form two coordinated, $\text{S}(2c)$ and one coordinated, $\text{S}(1c)$ atoms capping Mo atoms on the edges of the platelets, respectively. Note that in the bulk, each S atom is connected with 3 Mo atoms, while Mo atom binds with 6 S atoms. The parallelogram shaped (m,n) platelets, $m = 1$ to 6 and $n = m$ to 6, are constructed by ensuring no under-coordinated Mo atoms in it. The numbers of Mo and S atoms in a platelet are given by $m \times n$ and $2(m \times n + m + n)$, respectively. From this, the stoichiometry of a platelet (S/Mo ratio = $2[1 + 1/m + 1/n]$) is always higher than the value for the bulk phase (S/Mo ratio = 2).

The optimized geometries of (m,n) parallelogram platelets with $m = 1$ to 6 and $n = m$ to 6 are shown in Fig. 1. Among (1, n) platelets, the (1,1) platelet has C_{3v} symmetry (Fig. 3). In this structure, the Mo atom is surrounded by six S atoms (S/Mo ratio = 6) in a prism structure and the S atoms below and above the Mo atoms are paired forming altogether three dimers with a bond length of 2.01 Å . These dimers are separated with an inter-sulfur distance of 3.43 Å on one side of the platelet and 3.79 Å on the other side of the platelet. As a result, the corresponding Mo–S bond distances are 2.43 Å and 2.28 Å , respectively. In (1,2) platelet, the symmetry is absent due to the

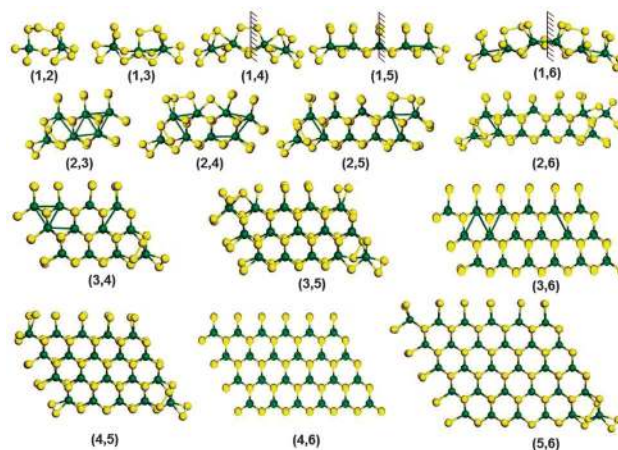


Fig. 1 Ball-and-stick models of the optimized structures of all (m,n) parallelogram shaped platelets. The green (yellow) balls correspond to Mo (S) atoms. The structures for platelets with $m = n$ are given in Fig. 3. Mirror symmetry is marked in some structures.

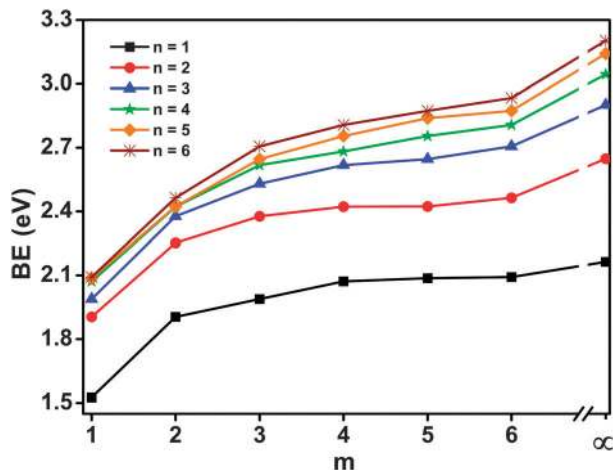


Fig. 2 BE of (m,n) parallelogram platelets along with the values for the corresponding MoS_{2+x} infinite nanoribbons. The values for (m,n) and (n,m) platelets are the same.

presence of a sulfur trimer in which the mean S–S distance is 2.1 Å. In addition, S(2c) and S(1c) atoms are bonded to Mo atoms with distances of 2.35 Å and 2.14 Å, respectively. This shows that S(1c) atoms which are the terminal S atoms, have a very short Mo–S bond length. The Mo–Mo distance is elongated to 3.8 Å from its bulk value of 3.17 Å due to the presence of S(1c) atoms. On the other hand, two Mo–Mo distances in the (1,3) platelet are 3.0 Å because these atoms do not have any S(1c) atom and there is significant dimerization of S atoms. Similar to the (1,2) platelet, no symmetry is present in this platelet because of the presence of the S trimer. Both (1,4) and (1,5) platelets have mirror symmetry because of the absence of S trimer. Note that even though trimer is present in the (1,6) platelet, the mirror symmetry is preserved as the trimers are distributed symmetrically in this structure (refer Fig. 1).

In $(2,n)$ platelets, the Mo atoms interact in two directions. Note that in all $(m > 2, n > 2)$ platelets, two adjoining edges have 100% S, while the other two edges have 50% S. In the (2,2) platelet (Fig. 3), there is a triangular metallic corner which is formed at the intersection of 100% S covered edges by three strongly interacting Mo atoms with the mean bond distance of 2.71 Å (Mo–Mo distance in bulk $\text{MoS}_2 = 3.17$ Å). It implies that the Mo atoms at this corner have enough charge to make strong Mo–Mo bonds. The mean Mo–Mo bond distance in the corner triangle of (2,2), (2,3), (2,4), (2,5), and (2,6) platelets is 2.71, 2.84, 2.96, 3.07, and 3.14 Å, respectively. Thus, the Mo–Mo bond distances in this triangular corner of $(2,n)$ platelets increases with n and approach the bulk value for higher n . The optimized structures of the platelets with $m > 2$ and $n > 2$ are also given in Fig. 1. They show the same structural features as reported above. As an example, the triangular corner is also found in $(3,n)$ platelets with slightly larger Mo–Mo bond distances that vary from 2.82 to 3.22 Å with increasing size. In this series of platelets, the Mo–Mo bond length reaches the maximum value of 3.22 Å for (3,5) platelet (see Fig. S1 in ESI†). In $(4,n)$ platelets, the trend is somewhat different. We do not find a triangular metallic corner for (4,4), (4,5), and (4,6)

platelets, as the Mo–Mo distance is always larger than the bulk value. Except for this series, the $m = n$ platelets always have the lowest Mo–Mo bond distance at the metallic corner in the respective series (refer ESI,† Fig. S1).

At the junction of 50% S covered edges, there is dimerization of sulfur atoms on one side of the plane of the platelet as can be seen in Fig. 3 while on the other side the bond length becomes elongated. Similarly at the junction of 50% and 100% S covered edges, there is dimerization of terminal sulfur atoms with some twisting. Also note that on the remaining two corners, the terminal sulfur atoms are dimerized but without twisting. This structural feature leads to an interesting variation in the magnetic moment on S atoms on the 50% S covered edges.

The binding energy per atom (BE) of various (m,n) platelets is obtained from

$$\text{BE} = \frac{(mn)E(\text{Mo}) + 2lE(\text{S}) - E(\text{Mo}_{mn}\text{S}_{2l})}{mn + 2l}$$

where, $l = mn + m + n$. $E(\text{Mo})$, $E(\text{S})$, and $E(\text{Mo}_{mn}\text{S}_{2l})$ are the total energies of a Mo atom, S atom, and (m,n) platelet, respectively. The calculated BE (Fig. 2) for the various platelets shows that it increases with size and approaches the maximum value for the corresponding (m, ∞) infinite nanoribbon in that series. On the other hand the S/Mo ratio in platelets decreases with increasing size and it approaches the bulk stoichiometry. It has been reported¹¹ that the triangular platelets with a S/Mo ratio of less than 3.5 could be synthesized in experiments. In parallelogram platelets two sides have 100% S while the other two sides have 50% S. Hence, the total number of edge S(1c) and S(2c) atoms in a parallelogram platelet is in between that of 50% and 100% S covered triangular platelets. Therefore, experimentally parallelogram platelets are likely to be formed in a lower sulfur environment.

The metallic behavior of the MoS_{2+x} platelets is driven by the edge states which lie around the HOMO. We find that the highest occupied molecular orbital–lowest unoccupied molecular orbital (HOMO–LUMO) gap of the platelets decreases with increasing size (Table 1) in an oscillatory manner and already for a (5,5) platelet, the gap becomes very small. Further *some of the platelets have magnetic moments that generally originate at the S(2c) atoms present on the 50% S covered edges rather than from Mo atoms*. In the case of the (1,1) platelet, there is a total magnetic moment of 2 μ_B . To understand the origin of magnetism in these platelets, we plotted the spin density distribution in Fig. 3 and it shows polarization on different sites. In the (1,1) platelet, the isosurface covers the whole cluster. In general, magnetism is expected to arise due to the presence of partially occupied 4d orbitals on Mo atoms as observed in the polyhedral MoS_2 clusters.²⁴ But in parallelogram shaped platelets it is not the case. In fact, magnetism could not be observed in the 100% S covered side of the platelets, but some of the S(2c) atoms and corner S(1c) atoms at the 50% S covered side possess magnetic moments. This is due to partial charge transfer to S atoms that lead to the 3p states of such S atoms partially unoccupied as shown in Fig. 4. Thus, we conclude that the spin-polarization is spatially localized on the 50% S covered edge of the platelets.

Table 1 The BE, magnetic moment (M), energy difference between the magnetic and non-magnetic solutions (ΔE), and HOMO–LUMO gap of (m,n) parallelogram platelets and the (m,∞) nanoribbons

(m,n)	Platelet	M (μ_B)	ΔE (eV)	BE (eV)	Gap (eV)
(1,1)	Mo ₁ S ₆	2.0	0.30	1.53	0.33
(1,2)	Mo ₂ S ₁₀	0.0	0.00	1.90	0.89
(1,3)	Mo ₃ S ₁₄	0.0	0.00	1.99	0.48
(1,4)	Mo ₄ S ₁₈	0.0	0.00	2.07	0.80
(1,5)	Mo ₅ S ₂₂	0.0	0.00	2.09	0.33
(1,6)	Mo ₆ S ₂₆	0.0	0.00	2.09	0.35
(1, ∞)	Mo ₁ S ₄	0.0	0.00	2.16	0.15
(2,2)	Mo ₄ S ₁₆	0.0	0.00	2.25	0.37
(2,3)	Mo ₆ S ₂₂	0.0	0.00	2.38	0.35
(2,4)	Mo ₈ S ₂₈	0.0	0.00	2.42	0.43
(2,5)	Mo ₁₀ S ₃₄	0.0	0.00	2.42	0.15
(2,6)	Mo ₁₂ S ₄₀	0.0	0.00	2.46	0.27
(2, ∞)	Mo ₂ S ₆	0.57	0.09	2.65	Metal
(3,3)	Mo ₉ S ₃₀	0.0	0.00	2.53	0.31
(3,4)	Mo ₁₂ S ₃₈	0.0	0.00	2.62	0.31
(3,5)	Mo ₁₅ S ₄₆	2.0	0.05	2.65	0.06
(3,6)	Mo ₁₈ S ₅₄	2.0	0.13	2.71	0.18
(3, ∞)	Mo ₃ S ₈	0.55	0.08	2.90	Metal
(4,4)	Mo ₁₆ S ₄₈	2.0	0.08	2.68	0.12
(4,5)	Mo ₂₀ S ₅₈	2.0	0.16	2.75	0.14
(4,6)	Mo ₂₄ S ₆₈	2.0	0.20	2.81	0.16
(4, ∞)	Mo ₄ S ₁₀	0.57	0.00	3.04	Metal
(5,5)	Mo ₂₅ S ₇₀	2.0	0.25	2.84	0.01
(5,6)	Mo ₃₀ S ₈₂	2.0	0.18	2.87	0.04
(5, ∞)	Mo ₅ S ₁₂	0.58	0.08	3.14	Metal
(6,6)	Mo ₃₆ S ₉₆	4.0	0.22	2.93	0.16
(6, ∞)	Mo ₆ S ₁₄	0.56	0.07	3.20	Metal

The electronic density of states (DOS) of a (6,6) platelet (Fig. 4) shows that the Mo-4d states are partially occupied, while S-3p states are almost fully occupied. We also observe strong p–d hybridization between Mo-4d and S-3p states in the DOS of all the platelets. Table 1 shows the magnetic moments (M), energy difference between the magnetic and non-magnetic solutions of different platelets (ΔE), binding energy (BE), and HOMO–LUMO gap (Gap) of all the platelets we have studied. There is a small gap of 0.16 eV for (6,6) platelet. However, the DOS curve shows no gap due to the Gaussian broadening of the electronic states (width = 0.1 eV). It is also observed that the exchange-splitting is there only in 3p states of some edge sulfur atoms (marked 1, 2, and 3 in Fig. 4) which lie near the HOMO. The difference in the energies of the magnetic and non-magnetic calculations is also small.

Our results suggest that the magnetic moments on some of the edge S(2c) atoms depend on the vertical (along the z-axis) separation between such S atoms. Therefore we explored the dependence of the magnetic behavior on the separation between the magnetic sulfur atoms lying on the edges. In (6,6) platelet, S(2c)–S(2c) separations at 1 and 2 sites (marked in Fig. 3) are 3.04 and 2.75 Å, respectively and the local moments on each S(2c) atom at the corresponding site are 0.26, and 0.35 μ_B suggesting an increase in the moments with a decrease in the separation between the S atoms. To understand further, we plotted the partial DOS of 3p states of these two magnetic S atoms and these are shown in Fig. 4b. The exchange-splitting for the 3p states near the E_{HOMO} of the respective magnetic S atoms are 0.47 and 0.60 eV. It shows that the exchange-splitting for S(2c) atoms also increases with

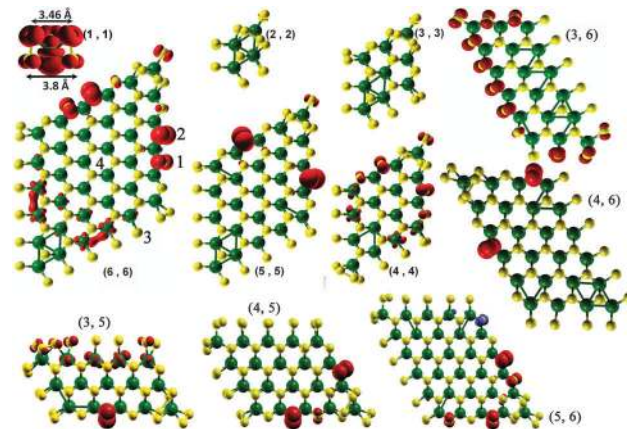


Fig. 3 Spin density distribution in the (m,n) platelets. The green (yellow) balls correspond to Mo (S) atoms. Isosurface value of $89 \times 10^{-3} \text{ e}^- \text{ \AA}^{-3}$ is used.

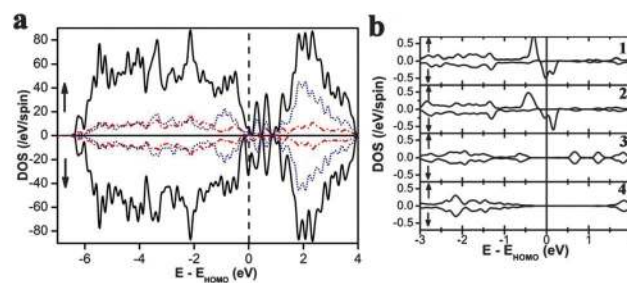


Fig. 4 (a) The total (black) and partial DOS (dotted blue and dashed red for Mo and S, respectively) of a (6,6) parallelogram platelet. (b) Partial DOS of 3p states of various S atoms shown as 1, 2, 3, and 4 in Fig. 3.

decreasing S(2c)–S(2c) separation. Note that a sulfur dimer has a 2 μ_B magnetic moment. In our case it is less as there is charge transfer from Mo atoms. The partial DOS of S(1c) and S(3c) atoms (marked 3 and 4 in (6,6) platelet in Fig. 3) are shown in Fig. 4b and it is seen that the 3p states of S(1c) and S(3c) atoms do not have any spin moment as a result of zero exchange-splitting. In the case of the sulfur dimer marked as 3, the S–S separation is 2.04 Å and it lies in between the values 1.97 Å for S₂ (2 μ_B) and 2.1 Å for S₂²⁻ (0 μ_B). Some change in the bond length occurs due to the interaction with Mo atoms. On the other hand, for the site marked 4, it is similar to that in bulk MoS₂ and the magnetic moment is zero.

In order to understand the magnetic behavior with respect to size, we have plotted the spin density for all the platelets having magnetic moments and these are shown in Fig. 3. It is understood that magnetism in parallelogram shaped platelets is localized primarily on sulfur atoms of the 50% S covered side irrespective of the lengths of the sides except for the (3,5) and (6,6) platelets in which case Mo atoms on the 100% S covered side also have some spin-polarization and it is due to the interdimer interactions but this effect is observed to be weak. Such a conclusion has also been obtained from earlier studies on triangular platelets by Zhang *et al.*¹⁶

We further plotted the charge density in the energy range of –0.7 to 0.0 eV (shown in Fig. 5a) as the states near the HOMO

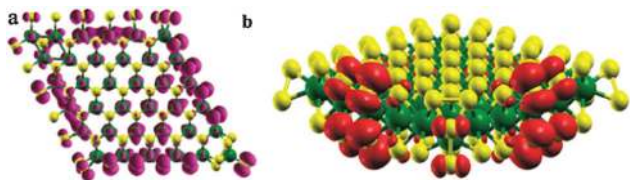


Fig. 5 (a) The partial charge density of (6,6) platelet from the states that lie in the energy range of -0.7 to 0.0 eV ($E_{\text{HOMO}} = 0.0$ eV) and (b) its spin-polarization distribution (rear view). The green (yellow) balls correspond to Mo (S) atoms. Note the tilted p_z orbitals on the 50% S covered edges.

are important for the catalytic activity of the platelets. Also the S atoms at the edges of the platelet contribute more in this energy range. This has been observed in the STM images of the triangular platelets as reported by Lauritsen *et al.*¹¹ Furthermore, our calculations evidently show (Fig. 5) that the 4d orbitals of the edge Mo atoms also contribute significantly in this region in the 100% S covered side, while on the 50% S covered edges, 3p orbitals of S(2c) atoms contribute significantly. Moreover, the 4d orbitals of interior (bulk-like) Mo atoms contribute significantly in this region in the triangular half platelet with 50% S covered edges. Therefore the effect of edges is felt more significantly in the interior of the platelet near the 50% S covered edges. This feature has been independently noticed in the STM images of the 100% and 50% S covered triangular platelets by Lauritsen *et al.* Such effects on Mo atoms in the interior of the platelets of 100% and 50% S covered sides will be diluted in large size platelets as the atomic environment of Mo atoms in the interior of the platelet becomes more as in the bulk.

It is also inferred from the charge density isosurface in Fig. 5a that the d_{xy} type orbital of the edge Mo atoms at the 100% S covered edge overlaps laterally with the same kind of orbital of the nearby Mo atoms. On the other hand, the p_z orbital of S(2c) atoms is slightly tilted at the 50% S covered edges as shown in Fig. 5b. Because of this, the S atoms may not be clearly visible in the scanning tunnelling microscope images¹¹ as also observed earlier in 50% S covered triangular platelets. However, in the interior of the platelet, we observe d_{z^2} orbital of some Mo atoms similar to the bulk. Whereas, the edge Mo atoms are not in the bulk like symmetry and are electronically modified by (100% and 50%) S decorations.

In order to understand magnetism on S(2c) atoms in parallelogram platelets, we performed first principles calculations on $(6, \infty)$ Mo_6S_{14} nanoribbons and the spin-polarization distribution at the equilibrium lattice constant is shown in Fig. S2 of ESI† This system is considered because the S–S bond distances could be varied by changing the lattice constant and its magnetic properties could be evaluated with self-consistent calculations. The total energy and the relaxed Mo–S and S–S bond distances obtained for various lattice constants as well as the S(2c)–S(2c) separation dependent magnetic moments are shown in Fig. 6. The equilibrium lattice constant of the $(6, \infty)$ nanoribbon is 3.15 Å. When the lattice parameter is increased, the Mo–S bond distance monotonically increases from 2.44 to 2.51 Å, whereas the S(2c)–S(2c) bond distance decreases significantly. However, it reaches the least value of 2.67 Å and further increasing the

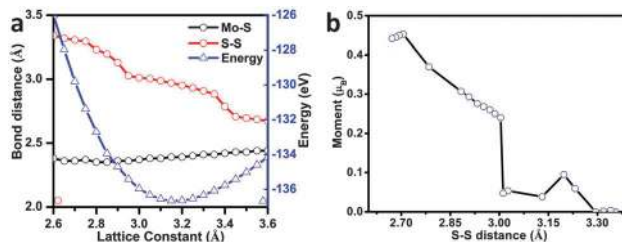


Fig. 6 (a) The total energy, and Mo–S as well as S(2c)–S(2c) bond distances for different lattice constants of $(6, \infty)$ MoS_{2+x} nanoribbons and (b) the magnetic moment as a function of S(2c)–S(2c) separation.

lattice constant does not change it (refer Fig. 6a). It is interesting to observe in Fig. 6b that the magnetism is highly dependent on S(2c)–S(2c) bond distances and it arises when this bond distance lies in between 2.69 and 3.0 Å (bulk S–S separation = 3.17 Å). Our results show that beyond the S(2c)–S(2c) separation of 3.0 Å, the magnetic interaction between S(2c) atoms is weak. Thus, we conclude that the magnetic moments in S(2c) atoms are present in parallelogram platelets when the separation between the S(2c) atoms lies in the range of 2.7 – 3.0 Å. In addition to the S(2c)–S(2c) distance, the edge Mo–Mo bond distance also plays a crucial role in magnetism of platelets. It is interesting to observe in Fig. S3 of ESI† that the magnetic moments in S(2c) atoms are present only when the separation between the two Mo atoms bonded with those S(2c) atoms lies above 3.1 Å. When Mo–Mo distance is less than 3.1 Å, the moments on S(2c) atoms are quenched along with that of the other S(2c) atoms, through strong Mo–Mo interactions. Thus, the Mo–Mo interaction also plays a crucial role in magnetic behavior of the parallelogram platelets.

In general, the magnetic moments on dimerized S(1c) atoms do not occur. There is strong overlap between the orbitals of those atoms and these dimers are in a nearly S_2^{2-} configuration which is non-magnetic. However, the S dimer located at the corner of the 50% S covered edges of a platelet has spin moments of $0.1 \mu_B$ for each S(1c) atom as can be seen from the isosurface of spin polarization in Fig. 5b. It is due to the occurrence of incomplete charge transfer from the Mo atom so that the 3p orbitals of these atoms remain partially unoccupied as shown in Fig. 4b. Fractional charge transfer to S atoms from Mo atoms is favorable in MoS_{2+x} platelets due to excess S atoms and this also leads to pairing of S atoms. As an example, in the (1,1) Mo_1S_6 platelet, the Mo atom is supposed to give all 6 electrons to three S dimers for forming S_2^{2-} species. In reality, the Mo atom keeps some charge (nearly $2/3 e^-$) in the d_{z^2} orbital and there is a resulting magnetic moment on the Mo atom (refer Fig. 3). Since the charge transfer to three S dimers is not complete, they also carry magnetic moment and the resultant magnetic moment in the Mo_1S_6 platelet is $2 \mu_B$. Therefore magnetism in the MoS_{2+x} platelet is primarily due to the occurrence of fractional charge transfer.

4 Conclusions

In summary we performed first principles calculations to understand the structural, electronic, and magnetic properties of MoS_{2+x}

parallelogram platelets. Our calculations show that a triangular metallic corner is obtained in the case of platelets with $m = n$, due to the presence of excess charge on Mo atoms. For platelets with a size greater than that of (3,5), magnetism is observed and it mainly arises from S(2c) atoms on 50% S covered edges rather than on Mo atoms. The criteria for magnetic moments on S(2c) atoms have been obtained and the separation between sulfur atoms plays an important role. It could be possible to manipulate magnetism in platelets by affecting the bond lengths. Our results show partial charge transfer from Mo atoms to sulfur atoms that results in partially unoccupied 3p states of those S atoms that give rise to magnetism. Similar to triangular platelets we also find brim states which lie near the HOMO of the platelets and have charge predominantly on the edges of the platelets and that are likely to be important for the catalytic activity of the platelets.

Acknowledgements

This work is supported by the Department of Science and Technology of India through Fast Track Scheme. J. Karthikeyan acknowledges the kind support and hospitality at Shiv Nadar University, where part of this manuscript was written. The calculations were performed at CSIR-CECRI, CSIR-NCL and CSIR-CMMACS HPC facilities.

References

- 1 P. Ball, *Nature*, 1991, **354**, 18; H. P. Schultz, *J. Org. Chem.*, 1965, **30**, 1361; A. K. Geim and K. S. Novoselov, *Nat. Mater.*, 2007, **6**, 183; M. S. Dresselhaus, G. Dresselhaus and P. C. Eklund, *Science of fullerenes and carbon nanotubes*, Academic press, 1996.
- 2 Y. Gogotsi, *J. Phys. Chem. Lett.*, 2011, **2**, 2509.
- 3 J. P. Salvetat, J. M. Bonard, N. H. Thomson, A. J. Kulik, L. Forr, W. Benoit and L. Zuppiroli, *Appl. Phys. A: Mater. Sci. Process.*, 1999, **69**, 255.
- 4 L. Li, R. Qin, H. Li, L. Yu, Q. Liu, G. Luo, Z. Gao and J. Lu, *ACS Nano*, 2011, **5**, 2601.
- 5 X. Wan, J. Dong and D. Y. Xing, *Phys. Rev. B: Condens. Matter*, 1998, **58**, 6756.
- 6 K. F. Mak, C. Lee, J. Hone, J. Shan and T. F. Heinz, *Phys. Rev. Lett.*, 2010, **105**, 136805.
- 7 A. Splendiani, L. Sun, Y. Zhang, T. Li, J. Kim, C.-Y. Chim, G. Galli and F. Wang, *Nano Lett.*, 2010, **10**, 1271; G. Eda, H. Yamaguchi, D. Voiry, T. Fujita, M. Chen and M. Chhowalla, *Nano Lett.*, 2011, **11**, 5111.
- 8 H. I. Karunadasa, E. Montalvo, Y. Sun, M. Majda, J. R. Long and C. J. Chang, *Science*, 2012, **335**, 698.
- 9 X. Zhang, B. Luster, A. Church, C. Muratore, A. A. Voevodin, P. Kohli, S. Aouadi and S. Talapatra, *ACS Appl. Mater. Interfaces*, 2009, **1**, 735.
- 10 Z. Wang, H. Li, Z. Liu, Z. Shi, J. Lu, K. Suenaga, S.-K. Joung, T. Okazaki, Z. Gu, J. Zhou, Z. Gao, G. Li, S. Sanvito, E. Wang and S. Iijima, *J. Am. Chem. Soc.*, 2010, **132**, 13840.
- 11 J. V. Lauritsen, J. Kibsgaard, S. Helveg, H. Topsoe, B. S. Clausen, E. Laegsgaard and F. Besenbacher, *Nat. Nanotechnol.*, 2007, **2**, 53.
- 12 S. Helveg, J. V. Lauritsen, E. Laegsgaard, I. Stensgaard, J. K. Nørskov, B. S. Clausen, H. Topsoe and F. Besenbacher, *Phys. Rev. Lett.*, 2000, **84**, 951.
- 13 Y. Shi, W. Zhou, A. Y. Lu, W. Fang, Y. H. Lee, A. L. Hsu, S. M. Kim, K. K. Kim, H. Y. Yang, L. J. Li, J. C. Idrobo and J. Kong, *Nano Lett.*, 2012, **12**, 2784.
- 14 J. Kibsgaard, B. S. Clausen, H. Topsoe, E. Laegsgaard, J. V. Lauritsen and F. Besenbacher, *J. Catal.*, 2009, **263**, 98.
- 15 M. Y. Sun, A. E. Nelson and J. Adjaye, *J. Catal.*, 2004, **226**, 32.
- 16 J. Zhang, J. M. Soon, K. P. Loh, J. Yin, J. Ding, M. B. Sullivan and P. Wu, *Nano Lett.*, 2007, **7**, 2370.
- 17 Y. Wua and H. Chen, *J. Magn. Magn. Mater.*, 2012, **324**, 2153.
- 18 G. Kresse and D. Joubert, *Phys. Rev. B: Condens. Matter Mater. Phys.*, 1999, **59**, 1758.
- 19 P. E. Blochl, *Phys. Rev. B: Condens. Matter*, 1994, **50**, 17953.
- 20 J. P. Perdew, J. A. Chevary, S. H. Vosko, K. A. Jackson, M. R. Pederson, D. J. Singh and C. Fiolhais, *Phys. Rev. B: Condens. Matter*, 1992, **46**, 6671.
- 21 L. Pauling, *The nature of the Chemical Bond*, Cornell University Press, 1960, vol. III, p. 175.
- 22 R. Krishnamurthy and W. B. Schaap, *J. Chem. Educ.*, 1969, **46**, 799.
- 23 A. Vojvodic, B. Hinnemann and J. K. Nørskov, *Phys. Rev. B: Condens. Matter Mater. Phys.*, 2009, **80**, 125416.
- 24 P. Murugan, V. Kumar, Y. Kawazoe and N. Ota, *Phys. Rev. A: At., Mol., Opt. Phys.*, 2005, **71**, 063203.